Supporting Information

Porous Graphene-Confined Fe–K as Highly Efficient Catalyst for CO_2 Direct Hydrogenation to Light Olefins

Tijun Wu,[†] Jun Lin,[‡] Yi Cheng,[†] Jing Tian,[†] Shunwu Wang,[†] Songhai Xie,[†] Yan Pei,[†] Shirun Yan,[†] Minghua Qiao,*[,†] Hualong Xu,[†] Baoning Zong*[,§]

[†]Collaborative Innovation Center of Chemistry for Energy Materials, Department of Chemistry and Shanghai Key Laboratory of Molecular Catalysis and Innovative Materials, Fudan University, Shanghai 200433, P. R. China

[‡]Key Laboratory of Nuclear Analysis Techniques, Shanghai Institute of Applied Physics, Chinese Academy of Sciences, Shanghai 201800, P. R. China

[§]State Key Laboratory of Catalytic Materials and Chemical Engineering, Research Institute of Petroleum Processing, SINOPEC, Beijing 100083, P. R. China

To whom correspondence should be addressed:

* Email: mhqiao@fudan.edu.cn (M. Q.)

* Email: zongbn.ripp@sinopec.com (B. Z.)

1. Materials

Li_2O (97%) and ZrO_2 (A.R.) were purchased from Aladdin. Silica sol (JN25, 25.0–26.0%) was purchased from Qingdao Haiyang. Nanosized TiO_2 (P25) was purchased from Beijing Boyu. Activated carbon (AC, Vulcan XC-72) was purchased from Carbot. Few-layer graphene oxide (GO) was purchased from Nanjing XFNANO. α-Al_2O_3, HCl (36.5 wt%), $Fe(NO_3)_3 \cdot 9H_2O$, and K_2CO_3, $N_2H_4 \cdot H_2O$ (85%), and anhydrous ethanol were of analytical grade (A.R.) and purchased from Sinopharm. The gases were all purchased from Shanghai Youjiali.

2. Catalyst Preparation

Synthesis of honeycomb-structured graphene (HSG). The HSG material was synthesized following the protocol raised by Hu and coworkers with some modifications.[1] About 15 g of Li_2O powders were loaded in a quartz boat and inserted into a quartz tube in a tube furnace. Under flowing CO of 50 ml min^{-1}, Li_2O was heated at a rate of 10 K min^{-1} from room temperature to 823 K and maintained for 24 h. After being cooled down to room temperature, the black powders was leached with diluted hydrochloric acid (5 wt%) to remove the formed Li_2CO_3 byproduct for 10 times, followed by washing with deionized water for another 10 times to neutrality. The centrifugation speed was 5000 rpm during acid leaching and water washing. Finally, the HSG material was obtained by drying at 353 K overnight.

Preparation of the Fe/HSG catalyst. Typically, 0.15 g of HSG was dispersed in 100 ml of deionized water by ultrasonication for 30 min to yield a black suspension. Under stirring, 0.27 g of $Fe(NO_3)_3 \cdot 9H_2O$ dissolved in 10 ml of deionized water was added. After the suspension was stirred at room temperature for 4 h, excessive water was evaporated at 333 K under stirring. The solid was further dried at 333 K in an oven for 12 h and calcined in Ar at 623 K for 4 h at a heating rate of 2 K min^{-1}.

Preparation of the Fe–K/HSG catalysts. The Fe–K/HSG catalysts were prepared by impregnating

the Fe/HSG catalyst with K_2CO_3. First, 0.20 g of the as-prepared Fe/HSG catalyst was reslurried in 100 ml of deionized water by ultrasonication. Then, a calculated volume of the K_2CO_3 aqueous solution (1 mg ml^{-1}) was added to give the prescribed K content. After the mixture was ultrasonicated for 30 min followed by stirring at room temperature for 4 h, excessive water was evaporated at 333 K under stirring. The solid was further dried at 333 K for 8 h in an oven. The as-prepared Fe–K/HSG catalysts were denoted as FeK0.5/HSG, FeK1/HSG, FeK1.5/HSG, FeK2/HSG, and FeK5/HSG depending on the nominal K contents of 0.50, 1.0, 1.5, 2.0, and 5.0 wt%, respectively.

Preparation of the control supported FeK1.5 catalysts. The preparation procedures of the FeK1.5/Al_2O_3, FeK1.5/TiO_2, FeK1.5/ZrO_2, and FeK1.5/AC were identical to those of the FeK1.5/HSG catalyst except for the difference in the support.

For the preparation of the FeK1.5/SiO_2 catalyst, 1.0 g of silica sol was added dropwise into 100 ml of aqueous solution containing 0.45 g of $Fe(NO_3)_3 \cdot 9H_2O$ under stirring. The slurry was stirred at room temperature for 4 h and then heated to 333 K for gelation. The gel was dried at 333 K for 12 h in an oven and pulverized. The Fe/SiO_2 catalyst was obtained by calcining the solid in Ar at 773 K for 4 h at a heating rate of 2 K min^{-1}. The following procedures for the preparation of the FeK1.5/SiO_2 catalyst were the same as those from the Fe/HSG catalyst to the FeK1.5/HSG catalyst.

For the preparation of the FeK1.5/rGO catalyst, GO was reduced with $N_2H_4 \cdot H_2O$ to rGO first.[2] Typically, 0.50 g of GO was dispersed in 100 ml deionized water under ultrasonication for 0.5 h to yield a yellowish-brown suspension. The suspension was further stirred at room temperature for 4 h and then heated to 363 K. Then, 10 ml of 85% $N_2H_4 \cdot H_2O$ was added dropwise and refluxed at 363 K for 12 h. The suspension was filtrated and washed with hot deionized water (363 K) for at least 5 times. The resulting black cake was dried at 333 K for 12 h in an oven and then pulverized. About 0.40 g of rGO was harvested, which was used as the support. The remaining procedures for the preparation of the

FeK1.5/rGO catalyst were the same as those from the Fe/HSG catalyst to the FeK1.5/HSG catalyst.

3. Characterization Techniques

N_2 physisorption was conducted at 77 K on a Micromeritics TriStar3000 apparatus. Prior to the measurement, the catalyst was heated at 473 K under flowing N_2 for 8 h. The Fe and K loadings were determined by inductively coupled plasma-atomic emission spectroscopy (ICP–AES; Thermo Elemental IRIS Intrepid).

The Raman spectrum was recorded at room temperature on a Horiba Jobin Yvon XploRA Raman spectrometer using a 12.5 mW laser source at an excitation wavelength of 532 nm. The spectral resolution was 1.8 cm^{-1}.

Powder X-ray diffraction (XRD) pattern was acquired on a Bruker AXS D8 Advance X-ray diffractometer using Ni-filtered Cu Kα radiation (λ = 0.15418 nm) equipped with a LynxEye 1-dimensional linear Si strip detector. The tube voltage was 40 kV, and the current was 40 mA. The 2θ angles were scanned from 20^o to 80^o at 1^o min^{-1} with a step of 0.01^o.

The surface morphology was observed on a Philips XL30 scanning electron microscope (SEM) operated at 50 kV. The catalyst was pasted on the conductive tape and then mounted on the sample stage. Both high-angle annular dark field (HAADF) image and transmission electron microscopic (HRTEM) image were observed on a Tecnai G^2 S-Twin F20 field-emission (S)TEM microscope operated at 200 kV. The catalyst, with the protection of anhydrous ethanol, was ground in an agate mortar and then diluted with anhydrous ethanol and ultrasonicated to homogeneity. The suspension was dripped onto a carbon film-coated copper grid. At least 200 particles were measured to construct the particle size distribution (PSD) histogram.

Temperature-programmed desorption (TPD) of H_2 and CO_2 was performed on a Micromeritics 2750

chemisorption system. Ar was used as the carrier gas during H_2-TPD, and He during CO_2-TPD. The weighed catalyst loaded in a U-shaped quartz tube was reduced at 723 K for 16 h in 5 vol% H_2/Ar (50 ml min^{-1}). After the sample was cooled to room temperature, H_2 or CO_2 pulses were injected until the eluted peak did not change in intensity, as monitored by a thermal conductivity detector (TCD). The catalyst was then purged with carrier gas (25 ml min^{-1}) for at least 30 min to remove the gaseous and physisorbed adsorbate until the baseline was restored. Desorption was conducted by heating the catalyst from room temperature to 723 K at 10 K min^{-1} and monitored by TCD. For the purpose of quantification, the area of the desorption peak was compared with that calibrated by a 100 μl-capacity loop using the corresponding adsorbate.

^{57}Fe Mössbauer absorption spectrum (^{57}Fe MAS) was recorded on a Wissel 1550 electromechanical spectrometer (Wissenschaftliche Elektronik GmbH) using a ^{57}Co in Pd matrix irradiation source in the constant acceleration transmission mode. The isomer shift (IS) was referenced to a 25 μm-thick α-Fe foil at room temperature. The spectrum was fitted using a least-squares fitting routine that modeled the spectrum as appropriate superpositions of quadruple doublets and magnetic sextets with Lorentzian line shape and constraints in peak width and intensity using the MossWinn 3.0i program. The contents of the iron-containing phases were derived from the areas of the absorption peaks with the assumption of the same recoil-free factor (the probability of absorption of the γ photons) for all kinds of iron nuclei in the catalyst.

4. Catalytic Testing and Product Analysis

The catalysts were pelletized, crushed, and sieved to 60–80 meshes. Prior to the reaction, 0.15 g of catalyst was diluted with 400 mg of powdered quartz (60–80 meshes) and activated on site in flowing CO (99.9%, 30 ml min^{-1}) at 623 K for 8 h with a heating rate of 2 K min^{-1}. Catalytic testing was performed

under the reaction conditions of 613 K, 2.0 MPa, and a $H_2/CO_2/N_2$ ratio of 72/24/4 by volume in a tubular fixed-bed reactor with an inner diameter of 10 mm. N_2 was used as the internal standard during gas-phase product analysis. To compare the product distribution at similar CO_2 conversion level, the gas hourly space velocity (GHSV) was adjusted depending on the activity of the catalyst. Specifically, the GHSVs were 13, 20, 41, 26, 20, and 14 l g^{-1} h^{-1} for the Fe/HSG, FeK0.5/HSG, FeK1/HSG, FeK1.5/HSG, FeK2/HSG, and FeK5/HSG catalysts, respectively.

The CO_2-FTO product analysis was conducted online using two gas chromatographs fixed with two high-temperature high-pressure Valco six-port valves. H_2, CO_2, N_2, CO, and CH_4 were analyzed on a GC122 gas chromatograph equipped with a 2 m-long TDX-01 packed stainless steel column connected to a TCD. The hydrocarbons were analyzed on a GC9560 gas chromatograph equipped with a PONA capillary column (50 m × 0.25 mm × 0.50 μm) connected to a flame ionization detector (FID). The olefins and paraffins of C_2–C_4 in the gas phase were additionally separated by a PoraPlot Q capillary column (12.5 m × 0.53 mm × 20 μm) connected to a FID on the GC122 gas chromatograph. The catalytic activity was expressed as iron time yield to hydrocarbons (FTY, moles of CO_2 converted to hydrocarbons per gram iron per second), and the productivity of light olefins ($FTY^{=}$) was expressed as moles of CO_2 converted to light olefins per gram iron per second. The hydrocarbon selectivities were calculated on a carbon basis with the exception of CO. The carbon balances of the CO_2-FTO products in all catalytic runs were within 95–98%.

Table S1. A Summary of the CO_2 -FTO Results over the Iron-Based Catalysts and Unconventional Non-Iron-Based Catalysts in the Literature

catalyst	*T* (K)	*P* (bar)	H_2/CO_2 (v/v)	GHSV ($l\ g^{-1}\ h^{-1}$)	CO_2 conv. (%)	FTY ($\mu mol_{CO2}\ g_{Fe}^{-1}\ s^{-1}$)	$FTY^{=}$ ($\mu mol_{CO2}\ g_{Fe}^{-1}\ s^{-1}$)	$C_2^{=}$–$C_4^{=}$ sel. (%)	CO sel. (%)	ref.
Fe–Co(0.17)/K(0.1)	573	11	3	3.6	31	14	8.0	58	18	[3]
K–Fe15	573	0.5	3	2.7	45	15	5.3	35	12	[4]
0.05MnFe	613	20	3	6	35	26	4.5	17	7.7	[5]
Fe–Na(1.18)	593	20	3	2	40	10	4.8	47	14	[6]
1Fe–1Zn–K	593	5	3	1	54	6.6	3.3	50	6.3	[7]
Fe_2O_3–CT600	573	10	3	1.2	23	3.4	1.1	32	n.a.[a]	[8]
KMnFe	573	18	3	2	41	10	5.1	50	12	[9]
Fe–Zr–Mn–K/TiO_2	573	10	3	1.3	25	3.9	1.5	38	n.a.[a]	[10]
Fe–K/Al_2O_3	573	10	3	1.8	31	2.4	1.4	59	n.a.[a]	[11]
K^+(1 wt%)Fe/ZrO_2	613	20	3	1.2	42	6.3	2.9	46	15	[12]
In_2O_3-β + SAPO-34	673	30	3	9	15	112[b]	86[b]	77	45	[13]
ZnZrO/SAPO	653	20	3	3.6	13	115[c]	103[c]	90	47	[14]
In–Zr/SAPO-34	613	20	3	9	35	82[d]	65[d]	80	85	[15]

[a]Not available. [b]Expressed in terms of the weight of In. [c]Expressed in terms of the weight of Zn and Zr. [d]Expressed in terms of the weight of In and Zr.

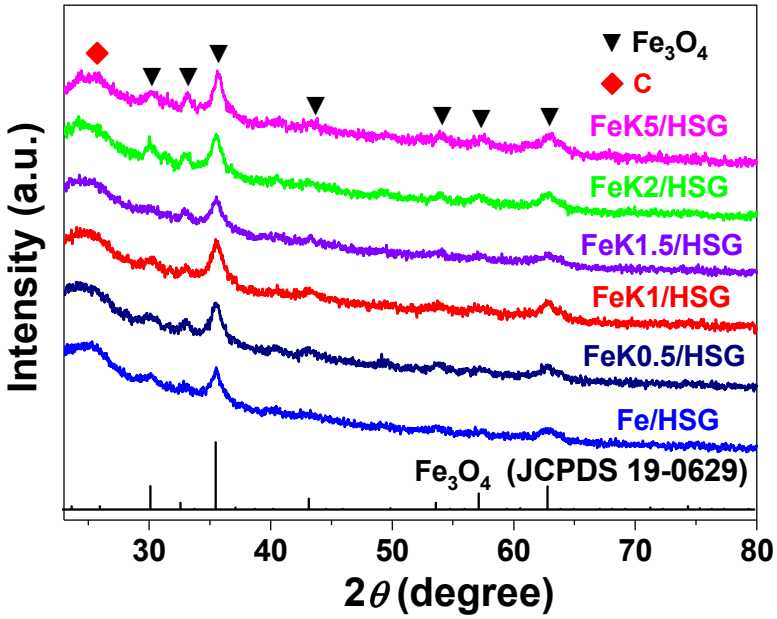

Figure S1. XRD patterns of the as-prepared Fe/HSG and Fe–K/HSG catalysts.

Table S2. Preliminary Physicochemical Properties of the Fe/HSG and Fe–K/HSG Catalysts

catalyst	Fe loading[a] (%)	K loading[a] (%)	S_{BET}[b] ($m^2\ g^{-1}$)	V_{pore}[b] ($cm^3\ g^{-1}$)	d_{pore}[b] (nm)	d_{Fe3O4}[c] (nm)	I_D/I_G[d]
Fe/HSG	18.3	/	110	0.48	14.6	9.1	1.11
FeK0.5/HSG	18.7	0.52	118	0.47	15.1	9.3	1.07
FeK1/HSG	17.9	1.03	121	0.47	15.3	10.2	1.11
FeK1.5/HSG	18.1	1.52	129	0.49	14.9	10.3	1.02
FeK2/HSG	17.4	2.02	137	0.48	14.7	11.5	1.05
FeK5/HSG	17.1	5.07	141	0.44	13.9	13.4	1.10

[a]Determined by ICP–AES. [b]Determined by N_2 physisorption. [c]Calculated by the Scherrer formula on the basis of XRD. [d]Raman intensity ratio between the D and G bands of graphene.

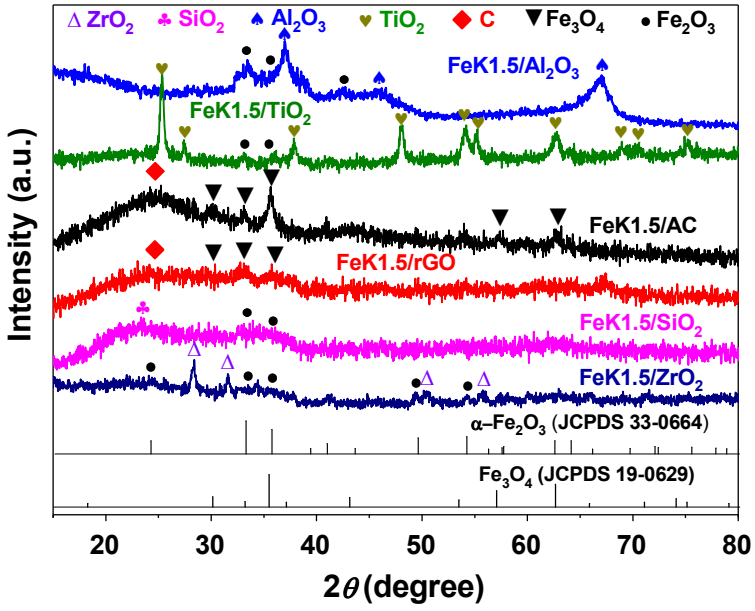

Figure S2. XRD patterns of the control FeK1.5 catalysts supported on various supports.

Table S3. Comparison of the CO_2 -FTO Results over the FeK1.5/HSG Catalyst and the Control Supported FeK1.5 Catalysts after 24 h on Stream

catalyst	*T* (K)	*P* (bar)	H_2/CO_2 (v/v)	GHSV ($l\ g^{-1}\ h^{-1}$)	CO_2 conv. (%)	FTY ($\mu mol_{CO2}\ g_{Fe}^{-1}\ s^{-1}$)	$FTY^{=}$ ($\mu mol_{CO2}\ g_{Fe}^{-1}\ s^{-1}$)	$C_2^{=}$–$C_4^{=}$ sel. (%)	CO sel. (%)
FeK1.5/HSG	613	20	3	26	46	123	73	59	44
FeK1.5/SiO_2	613	20	3	2.7	34	12	4.8	40	22
FeK1.5/Al_2O_3	613	20	3	3.4	42	17	11	63	30
FeK1.5/TiO_2	613	20	3	6.7	39	33	19	58	27
FeK1.5/ZrO_2	613	20	3	3.1	27	11	4.1	37	25
FeK1.5/AC	613	20	3	12	36	47	25	53	37
FeK1.5/rGO	613	20	3	22	37	76	43	56	46

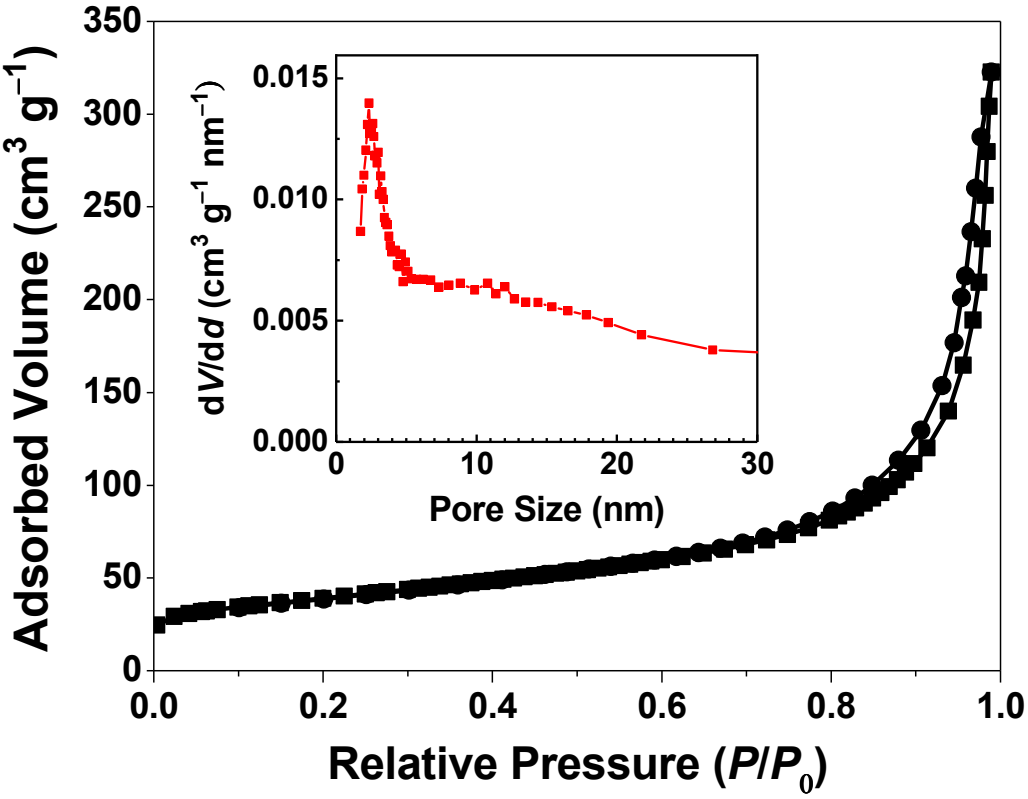

Figure S3. N_2 physisorption isotherms and pore size distribution of the FeK1.5/AC catalyst.

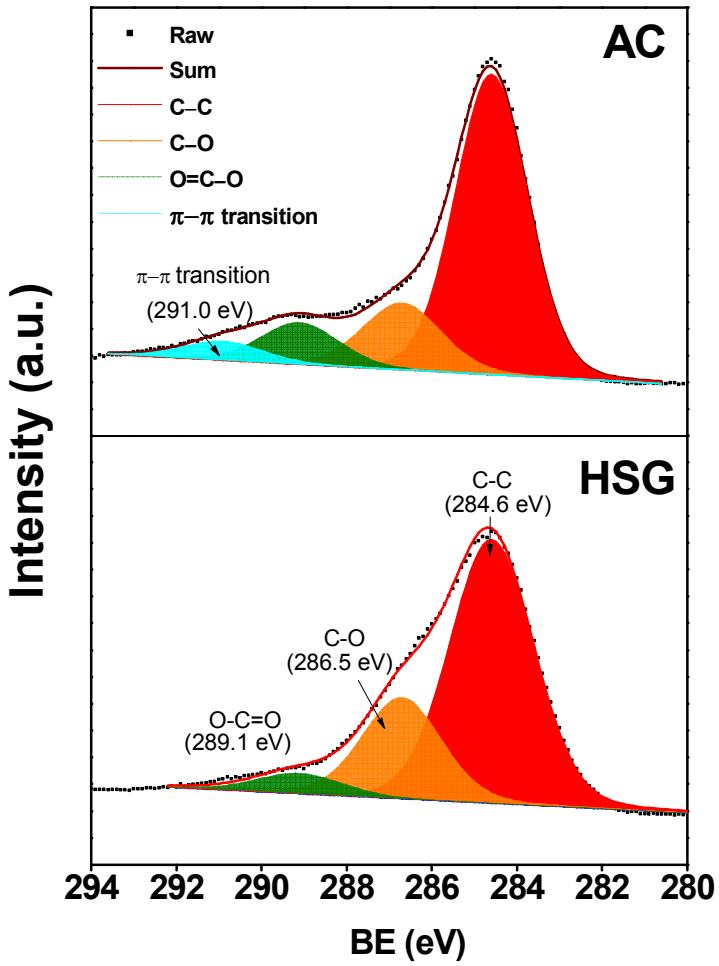

Figure S4. The C 1s spectra of AC and HSG.

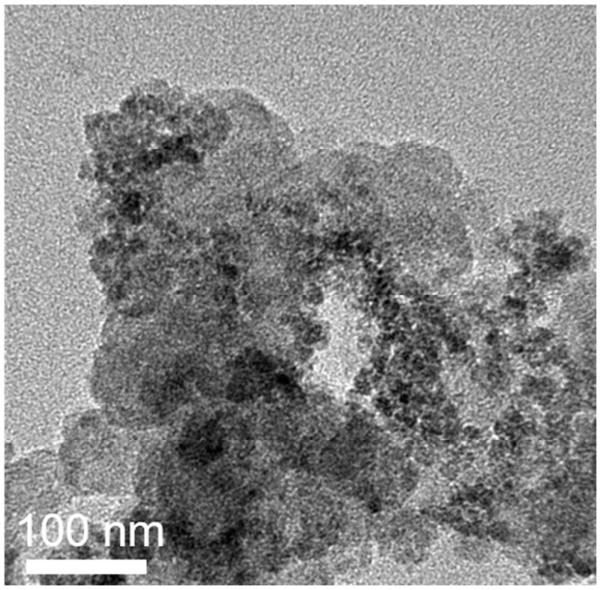

Figure S5. TEM image of the as-prepared FeK1.5/AC catalyst.

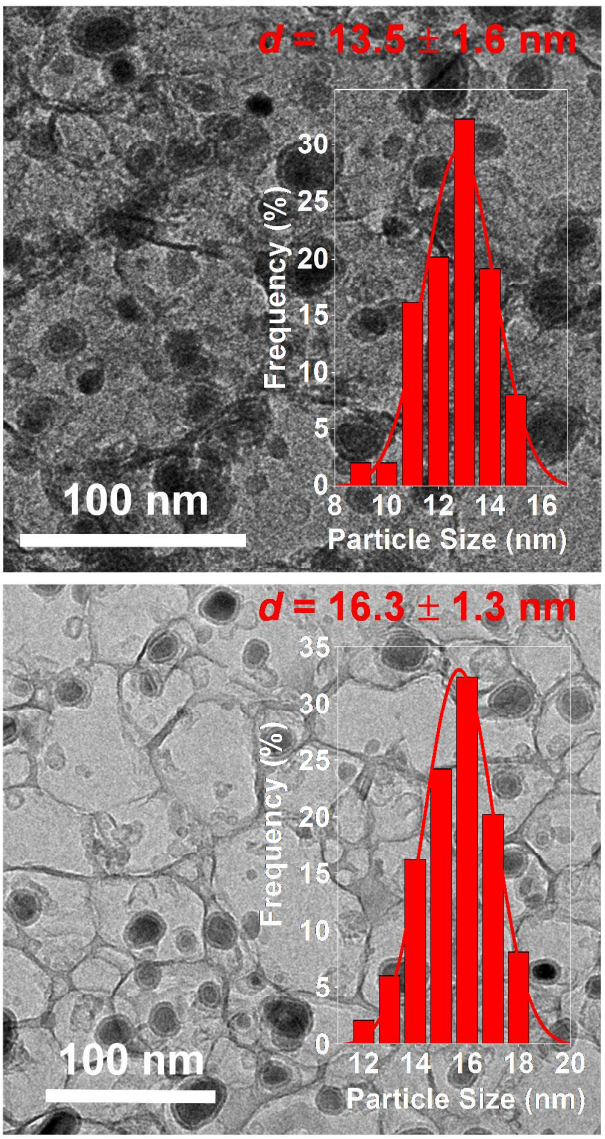

Figure S6. TEM images and particle size distribution histograms of (a) the as-prepared FeK1.5/rGO catalyst (top) and (b) the catalyst after 24 h on stream in CO_2-FTO (bottom).

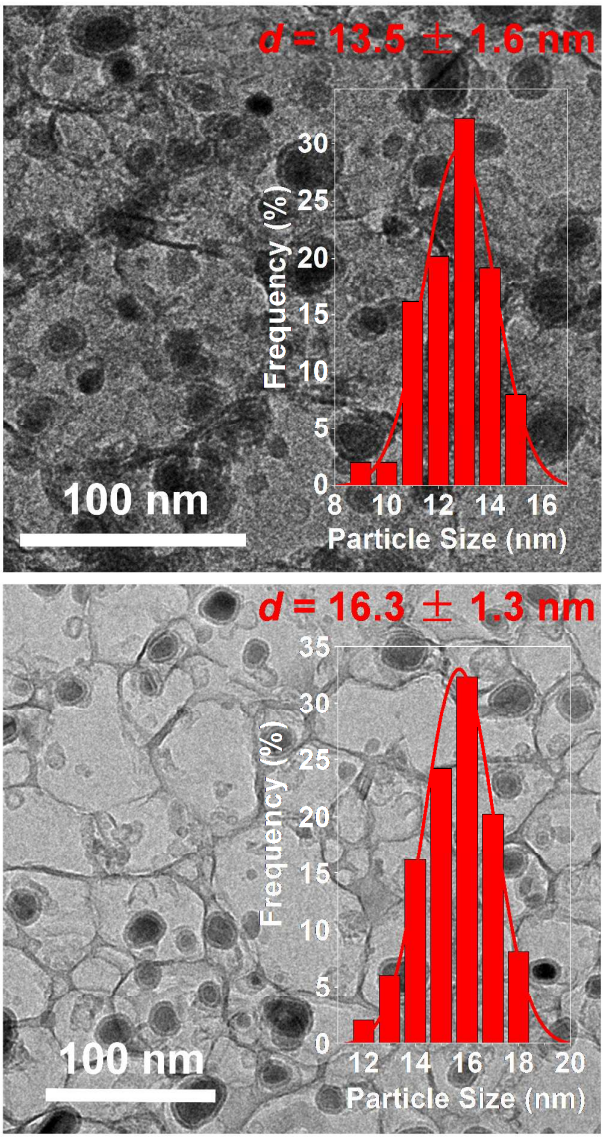

Figure S7. TEM images and particle size distribution histograms of the FeK1.5/HSG catalyst after (a) 24 h (top) and (b) 120 h on stream in CO_2-FTO (bottom).

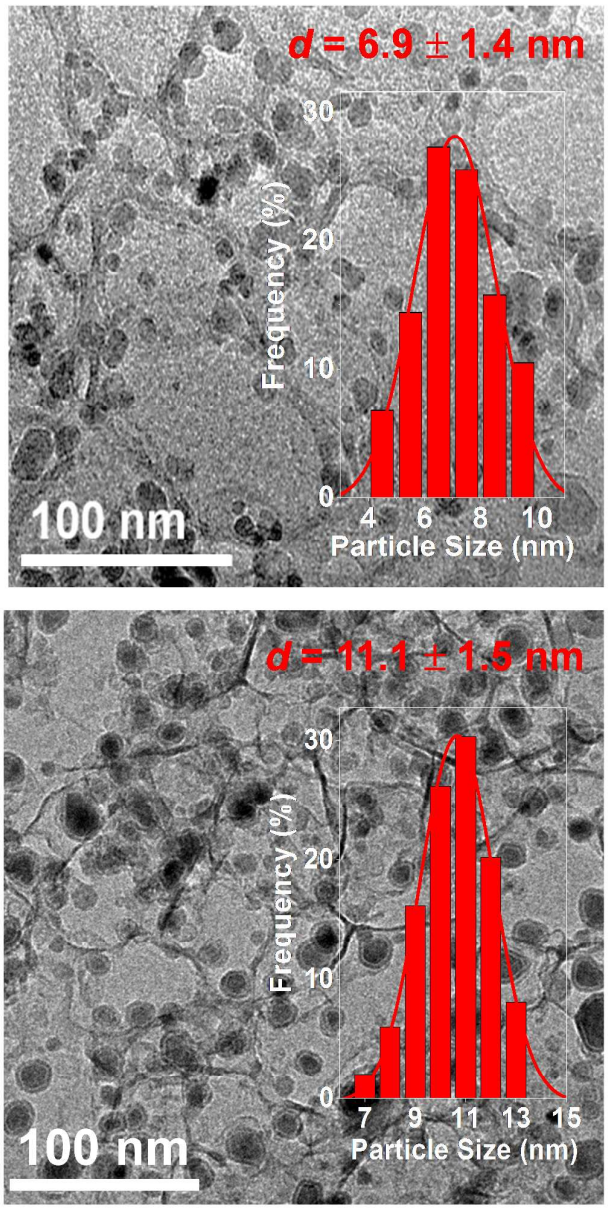

Figure S8. TEM images and particle size distribution histograms of (a) the as-prepared Fe/HSG catalyst (top) and (b) the catalyst after 24 h on stream in CO_2-FTO (bottom).

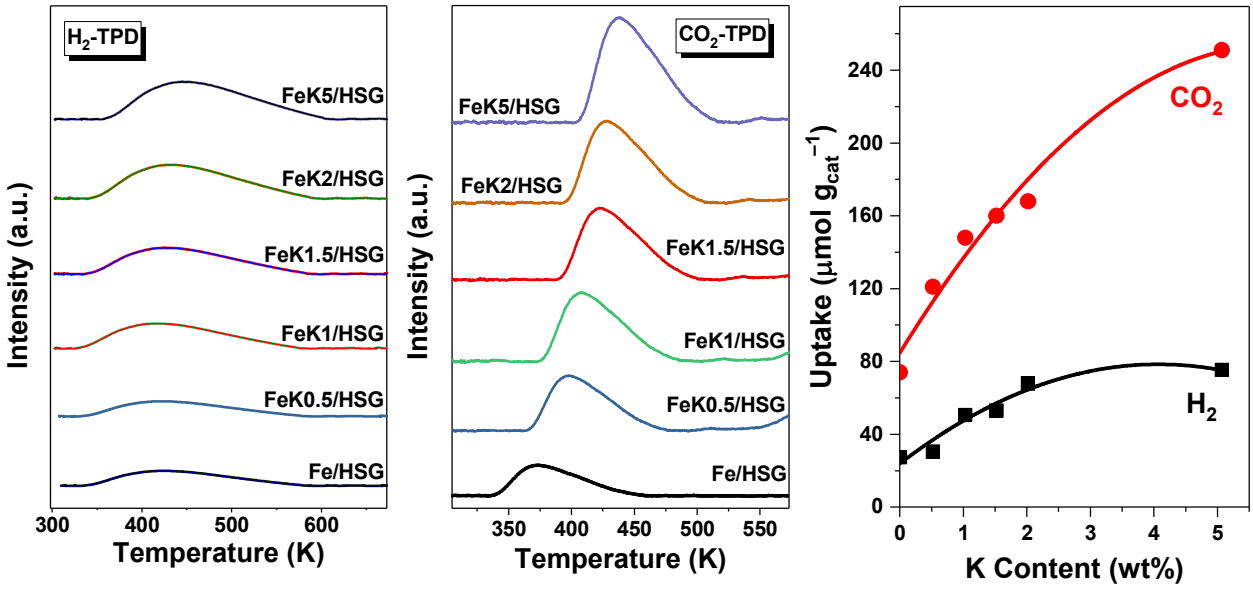

Figure S9. The H_2- and CO_2-TPD profiles and adsorption capacities of H_2 and CO_2 against the content of potassium on the Fe–K/HSG catalysts.

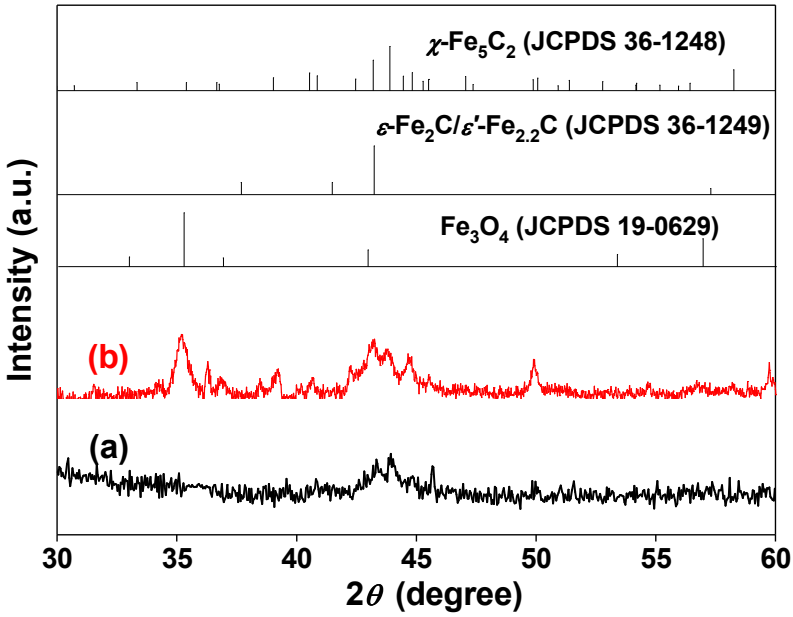

Figure S10. XRD patterns of the FeK1.5/HSG catalyst after (a) 24 h and (b) 120 h on stream in CO_2-FTO.

Table S4. ^{57}Fe Mössbauer Parameters of the Fe/HSG and FeK1.5/HSG Catalysts after CO_2-FTO[a]

catalyst	IS (mm s^{-1})	QS (mm s^{-1})	H (T)	Γ (mm s^{-1})	phase ascription	A (%)
Fe/HSG	0.96	0.28	/	0.69	low-coordination Fe(II)	31.9
after 24 h on	0.16	0.08	18.1	0.35	Fe_5C_2 (A)	9.3
stream	0.25	0.05	21.7	0.85	Fe_5C_2 (B)	29.7
	0.19	0.02	10.5	0.45	Fe_5C_2 (C)	11.4
	1.21	1.82	/	0.25	high-coordination Fe(II)	17.7
FeK1.5/HSG	0.31	1.05	/	0.69	Fe(III)	17.2
after 24 h on	0.15	0.04	18.3	0.41	Fe_5C_2 (A)	19.6
stream	0.26	0.04	21.7	0.57	Fe_5C_2 (B)	37.9
	0.22	0.08	10.9	0.48	Fe_5C_2 (C)	16.8
	0.21	0.19	16.4	0.36	$Fe_{2.2}C$	8.5
FeK1.5/HSG	0.44	0.81	/	0.94	Fe(III)	7.9
after 120 h	0.38	0.02	21.6	0.23	Fe_5C_2 (A)	23.8
on stream	0.25	0.08	18.0	0.27	Fe_5C_2 (B)	26.8
	0.32	0.23	10.7	0.18	Fe_5C_2 (C)	13.9
	0.85	/	44.0	0.15	Fe_3O_4 (I)	7.8
	0.20	0.08	17.9	0.38	$Fe_{2.2}C$	19.8

[a]IS, isomer shift (relative to α-Fe); QS, quadrupole splitting for doublet or quadrupole shift for sextet; H, hyperfine magnetic field; Γ, FWHM; A, relative spectral area.

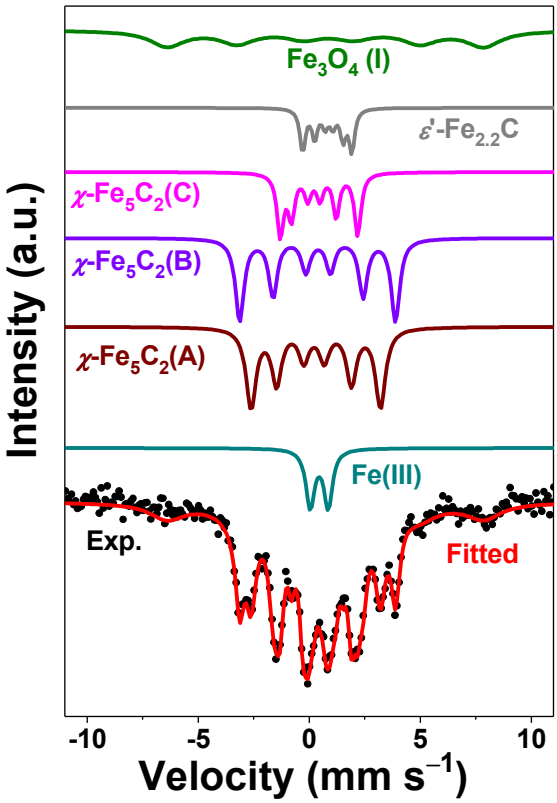

Figure S11. ^{57}Fe Mössbauer spectrum of the FeK1.5/HSG catalyst after 120 h on stream in CO_2-FTO.

References

[1] Wang, H.; Sun, K.; Tao, F.; Stacchiola, D. J.; Hu, Y. H. *Angew. Chem. Int. Ed.* **2013**, *52*, 9210–9214.

[2] Stankovich, S.; Dikin, D. A.; Piner, R. D.; Kohlhaas, K. A.; Kleinhammes, A.; Jia, Y.; Wu, Y.; Nguyen, S. T.; Ruoff, R. S. *Carbon* **2007**, *45*, 1558−1565.

[3] Satthawong, R.; Koizumi, N.; Song, C.; Prasassarakich, P. *J. CO_2 Util.* **2013**, *3–4*, 102–106.

[4] Visconti, C. G.; Martinelli, M.; Falbo, L.; Infantes-Molina, A.; Lietti, L.; Forzatti, P.; Iaquaniello, G.; Palo, E.; Picutti, B.; Brignoli, F. *Appl. Catal. B* **2017**, *204*, 119–126.

[5] Al-Dossary, M.; Ismail, A.; Fierro, J. L. G.; Bouzid, H.; Al-Sayari, S. A. *Appl. Catal. A* **2015**, *165*, 651–660.

[6] Wei, J.; Sun, J.; Wen, Z. Y.; Fang, C. Y.; Ge, Q. J.; Xu, H. Y. *Catal. Sci. Technol.* **2016**, *6*, 4786–4793.

[7] Zhang, J. L.; Lu, S. P.; Su, X. J.; Fan, S. B.; Ma, Q. X.; Zhao, T. S. *J. CO_2 Util.* **2015**, *12*, 95–100.

[8] Albrecht, M.; Rodemerck, U.; Schneider, M.; Broring, M.; Baabe, D.; Kondraterko, E. V. *Appl. Catal. B* **2017**, *204*, 119–126.

[9] Willauer, H. D.; Ananth, R.; Olsen, M. T.; Drab, D. M.; Hardy, D. R.; Williams, F. W. *J. CO_2 Util.* **2013**, *3–4*, 56–64.

[10] Rodemerck, U.; Holena, M.; Wagner, E.; Smejkal, Q.; Barkschat, A.; Baerns, M. *ChemCatChem* **2013**, *5*, 1948–1955.

[11] Lee, S. C.; Jang, J. H.; Lee, B. Y.; Kang, M. C.; Kang, M.; Choung, S. J. *Appl. Catal. A* **2003**, *253*, 293–304.

[12] Wang, J. J.; You, Z.; Zhang, Q. H.; Deng, W. P.; Wang, Y. *Catal. Today* **2013**, *215*, 186–193.

[13] Gao, P.; Li, S. G.; Bu, X. N.; Dang, S. S.; Liu, Z. Y.; Wang, H.; Zhong, L. S.; Qiu, M. H.; Yang, C. G.; Cai, J.; Wei, W.; Sun, Y. H. *Nat. Chem.* **2017**, *9*, 1019–1024.

[14] Li, Z. L.; Wang, J. J.; Qu, Y. Z.; Liu, H. L.; Tang, C. Z.; Miao, S.; Feng, Z. C.; An, H. Y.; Li, C. *ACS Catal.* **2017**, *7*, 8544−8548.

[15] Gao, P.; Dang, S. S.; Li, S. G.; Bu, X. N.; Liu, Z. Y.; Qiu, M. H.; Yang, C. G.; Wang, H.; Zhong, L. S.; Han, Y.; Liu, Q.; Wei, W.; Sun, Y. H. *ACS Catal.* **2018**, *8*, 571–578.